Palaeogeography, Palaeoclimatology, Palaeoecology 271 (2009) 69–76

Contents lists available at ScienceDirect

Palaeogeography, Palaeoclimatology, Palaeoecology

journal homepage: www.elsevier.com/locate/palaeo

Reinterpretation of palmate and semi-palmate (webbed) fossil tracks; insights from finite element modelling

Peter L. Falkingham [a,*], Lee Margetts [a,b], Ian M. Smith [c], Phillip L. Manning [a,d]

[a] University of Manchester, School of Earth, Atmospheric and Environmental Sciences, Williamson Building, Oxford Road, Manchester, M13 9PL, England, United Kingdom
[b] University of Manchester, Research Computing, England, United Kingdom
[c] University of Manchester, School of Mechanical, Aerospace and Civil Engineering, England, United Kingdom
[d] The Manchester Museum, University of Manchester, England, United Kingdom

ARTICLE INFO

Article history:
Received 26 March 2008
Received in revised form 1 August 2008
Accepted 15 September 2008

Keywords:
Cretaceous
Footprint
Track
FEA
Bird
Dinosaur

ABSTRACT

A track from the Late Cretaceous previously described as being generated by a semi-palmate bird was studied with the aid of high resolution laser scanning. Substrate conditions at the time of track formation were diagnosed (fine-grained, soft, waterlogged sediment) and used to constrain a finite element track simulator. The indentation of a non-webbed virtual tridactyl foot in such conditions created a resultant track with features analogous to 'webbing' between digits. This 'webbing' was a function of sediment deformation and subsequent failure in 3D, specific to rheology. Variation of substrate conditions and interdigital angle was incrementally stepped. Apparent webbing impressions were clearly developed only within a limited range of sediment conditions and pedal geometry.

The implications of this work are that descriptions of 'webbed' tracks should account for the possibility that webbing was indirectly formed through sediment failure and not necessarily the direct impression of a webbed foot. Additionally, dating the earliest occurrence of webbed feet in the fossil record, and potentially extending phylogenetic ranges, should be treated with caution when based upon evidence from tracks.

1. Introduction

Fossil vertebrate tracks are a source of information on the size, speed, limb kinematics and even behaviours of the animals that made them (Day et al., 2004; Manning, 2004 and references therein). In many cases, the fossil tracks provide information that is not preserved in skeletal remains. The record of palmate and semi-palmate (webbed) Cretaceous birds, for instance, is almost exclusively ichnological (Yang et al., 1995; Lockley and Rainforth, 2002; Lockley et al., 2004), with only a single web-footed specimen described to date (You et al., 2006).

Records of webbed bird tracks extend into the Early Cretaceous (Lim et al., 2000; Kim et al., 2006), and thereafter are not uncommon (e.g. Yang et al., 1995; Lockley and Rainforth, 2002; Lockley et al., 2004). The appearance of webbed bird tracks at this time has been interpreted as evidence of a considerable diversification of shore birds.

Sarjeant (1967) described a number of tracks from the Middle Triassic of Mapperly Park, Nottingham (UK) and described *Swinnertonichnus* as a small theropod track that displayed webbing, a feature not currently reported in body fossils of dinosaurs. These tracks were reinterpreted by King and Benton (1996) who observed no such evidence of webbing, noting that if substrate conditions were good enough to preserve interdigital webbing, claw impressions should also be present.

Track morphology is dependant upon a number of interacting factors, including limb kinematics, limb morphology and substrate properties. Once exposed, a track is subjected to the effects of weathering and erosion, which may further modify the geometry (Bates, 2006; Henderson, 2006; Bates et al., 2008). In order to recover information regarding the trackmaker, the interaction of these factors must be taken into account. These controlling factors will vary with sediment particle size and distribution, density, along with the air and/or water occupying the pore spaces between the particles. A clear example of this is demonstrated when water content is increased, reducing the amount of air filling the voids, resulting in the sediment volume becoming less compressible. The bulk density of the sediment increases, as does the shear strength, until the critical saturation point is reached, water then begins to push the particles apart, and the sediment fails (Karafiath and Nowatzki, 1978). In terms of track formation, a waterlogged sediment would prove soft, and easily deformed, but the incompressibility would lead to sediment being forced upwards around the foot to form displacement rims (Manning, 2004).

The effects of the limb–sediment interaction impact heavily upon the *volume* of sediment, and not just the surface in contact with the foot (Allen, 1989, 1997; Manning, 1999, 2004; Milàn et al., 2004; Milàn, 2006; Milàn and Bromley, 2006, 2008; Manning et al., in review). The

* Corresponding author. Fax: +44 1612753947.
E-mail address: Peter.Falkingham@manchester.ac.uk (P.L. Falkingham).

0031-0182/$ – see front matter © 2008 Elsevier B.V. All rights reserved.
doi:10.1016/j.palaeo.2008.09.011

consequence of this is that a track must be treated as a full three-dimensional volume, and not simply a surface feature representing the two-dimensional outline of the trackmaker's foot. Force will not only be transmitted downwards below the foot, but also out and up as sediment moves along the path of least resistance, according to Rankine's theory of shear (Craig, 1997; Manning, 2004).

The primary implications of complex deformation generated by a dynamic load are that tracks may appear substantially different to the morphology of the trackmaker's foot, depending on such conditions as those listed above, as well as which track surface within the volume is exposed. The fossil track collection at the Amherst College Museum of Natural History contains numerous examples where this is the case, with single trackways containing traces with varying numbers of digits, or individual tracks preserved as 'books' where several layers of rock have been peeled apart to reveal subsurface features. Each 'page' of the book may have a considerably different morphology to the last (Margetts et al., 2006; Manning et al., in review).

The 3D nature of tracks has been the focus of analogue modelling by track workers over the past decade (Allen, 1989, 1997; Manning, 1999, 2004; Milàn et al., 2004; Milàn, 2006; Milàn and Bromley, 2006; Manning, 2008; Milàn and Bromley, 2008). Such work has provided a quantitative approach to investigating the effects of substrate properties on track morphology, at the surface and within the sediment volume. Such physical modelling, however, is time consuming and in many cases requires physical sectioning and extraction of subsurface layers within the volume. This extraction process is destructive, disrupting the relative position of track surfaces within the volume.

The advance of computer power, combined with software design that takes advantage of multiple processors simultaneously, means that complex simulations such as the deformation of a substrate volume under dynamic loading conditions can be run to completion in feasible time frames. Such a simulation has many advantages over physical modelling, including precise and independent control of variables, and complete freedom to view a structure in three (or even four) dimensions non-destructively.

With this in mind we aim to test the hypothesis that web-like features may be formed as a function of sediment, and not automatically assumed to be of semi-palmate/palmate origin. A comparison of fossil tracks and finite element modelling (FEA) of substrate under dynamic loading is used herein to test this hypothesis.

1.1. The finite element method

Finite element analysis (FEA) is a numerical analysis technique common in engineering for exploring the mechanics of continuous media, though the method is applicable to a broad variety of mathematical problems that arise in almost all areas of science (Burnet, 1987; Smith and Griffiths, 2004). In simple terms, the method approximates the governing equations of a continuous system by dividing the continuum into 'finite elements.'

Many palaeontologists will primarily associate FEA with its use in testing load and subsequent stress within bones (Rayfield et al., 2001; Rayfield, 2004, 2005). Rayfield (2007) provides a review of the uses of FEA in palaeontology and also of the method itself.

A volume of sediment is composed of individual grains (of varying size and form), as well as water and air in pore spaces. However, a given volume of sediment, sufficiently large in relation to its constituent grains, can be considered as a single entity. This entity will have properties that define its behaviour under load (assuming homogeneity, heterogeneous volumes can be treated as 'blocks' of differing homogeneous volumes). As such, a volume of sediment can be treated as a continuum, and studied using FEA. This has been the case in the engineering fields for several decades, and the use of FEA for solving problems involving soils and sediments is now common place; for example, soil settlement (Scheiner et al., 2006), tire–soil interaction (Nakashima and Wong, 1993; Shoop, 2001; Fervers, 2004; Nakashima and Oida, 2004; Shoop et al., 2006) and building foundation problems (Johnson et al., 2006). A framework is therefore in place for defining and solving problems of soil deformation under load. This framework can be used to study vertebrate track formation.

2. Materials and methods

2.1. Fossil track

The specimen used as an example of a semi-palmate track was a cast of *Sarjeantopodus semipalmatus* (Lockley et al., 2004). The original fossil is held in the collections of the University of Colorado Dinosaur Tracks Museum (specimen no: CU-MWC224.4). The original locality was in eastern Wyoming, (U.S.A.), though was located on private land so exact locality data is withheld (Lockley et al., 2004). Found in the Late Cretaceous Lance Formation, the track horizon was located as casts on the underside of a 0.1 m thick, fine-grained sand/mud layer, situated a few centimetres above a major dinosaur track layer (Lockley and Rainforth, 2002; Lockley et al., 2004). The track horizon where CU-MWC224.4 was located also preserved raindrop impressions and small ripples.

In addition to the specimen (cast), a hand held laser scanner was used to generate a 3D digital surface of the track. The scanner used was a Polhemus FastScan Cobra capable of achieving >0.1 mm resolution. This allowed virtual manipulation of the track, including viewing the surface as an impression rather than a cast, and also allowing profile sections to be taken non-destructively. A digital representation of the track was directly compared with a surface generated by the FEA.

2.2. Finite element simulations

The software used herein was developed in-house, being a modified version of a three-dimensional finite element program in Smith and Griffiths (2004). The program uses a von Mises elasto-plasticity model to represent the plastic behaviour of the sediment.

A relatively simple cuboid mesh was created from hexahedral elements, each defined by eight nodes. To increase efficiency and decrease run time whilst maintaining a high resolution output, a scaling factor produced larger elements away from the source of loading (the 'foot'), and smaller elements beneath the load where deformation would be most intense and complex. The simulation was run at the meter scale for ease of use, though the results are directly scalable. The mesh measured 2 m×2 m at the surface, and was 1 m deep. This large size prevented any boundary effects caused by fixed nodes at the edges of the soil volume. Whilst the elements were arranged in 1 cm layers, these layers were given uniform properties creating a homogeneous sediment.

Loading was achieved through the direct displacement of surface nodes defining a track outline. The outline represents a generic tridactyl foot measuring 0.6 m in length (Fig. 1).

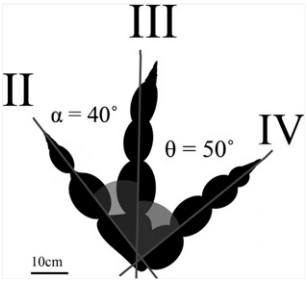

Fig. 1. Outline used to represent tridactyl foot. Interdigital angle (IDA) between Digits II and III — 40°, IDA between Digits III and IV — 50°. Foot length=60 cm.

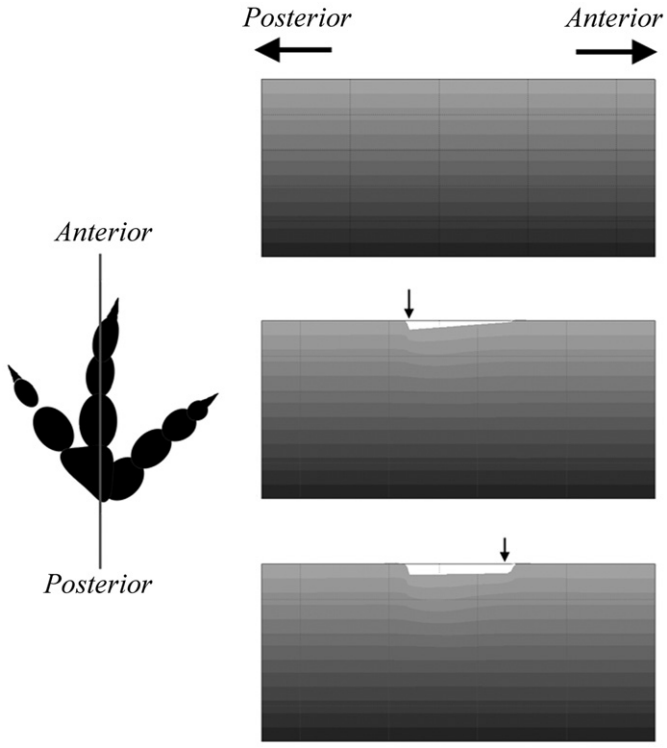

Fig. 2. Three cross-sections through a soil volume undergoing dynamic loading (top — prior to loading; centre — after 'heel' nodes are displaced; bottom — after full loading cycle). Sections are taken as indicated by the line through the track on the left.

The nodes were displaced in such a manner that the most posterior nodes (those forming the rear of the virtual foot) were vertically displaced first, followed by the anterior nodes (Fig. 2). This approximated a heel–toe step cycle where the centre of mass passes anteriorly over the foot, as opposed to a static loading scenario in which all nodes are displaced uniformly, a difference comparable to that between an animal standing still on a sediment, and an animal walking over that sediment. Manning et al. (in review) showed the difference in results obtained from static and dynamic loading regimes, where the dynamic loading produced more extensive zones of shear and deformation than static loading.

The sediment was defined by three parameters: undrained shear strength (u), Young's modulus (E) and Poisson's ratio (v). The undrained shear strength controls the stiffness and resistance of the sediment to shearing, the Young's modulus is the modulus of elasticity, and the Poisson's ratio is the measure of compressibility (the ratio of compression in one axis to extension along the normal axis), with 0.5 being incompressible and 0 being entirely compressible. Typical values for shear strength and Poisson's ratio are given in Tables 1 and 2 respectively. The Young's modulus varies and is defined according to these parameters.

Table 1
Undrained strength classification of clays according to BS 8004:1986 (from Craig, 1997)

Consistency	Undrained strength (kN/m^2)
Very stiff or hard	>150
Stiff	100–150
Firm to stiff	75–100
Firm	50–75
Soft to firm	40–50
Soft	20–40
Very soft	<20

Table 2
Typical values for Poisson's ratio in various substrates (from Bowles, 1968)

Material	Typical values for Poisson's ratio
Saturated clay	0.4–0.5
Rock	0.1–0.4
Sand, gravely sand	0.3–0.4
Silt	0.3–0.35
Sandy clay	0.2–0.3
Loess	0.1–0.3

The properties used for the experiment were chosen to represent a waterlogged fine sand/mud such as that found at the side of a body of water, following the palaeoenvironment and sedimentological interpretation offered by Lockley et al. (2004). As such, a high Poisson's ratio was used: v=0.499, and a low shear strength: u=45 kN/m^2 consument to the sediment conditions prevailing at the time of track formation (Lockley et al., 2004).

Saturated sediment, by definition, has a large amount of pore water occupying intergranular spaces. The relative incompressibility of water compared with the air it has replaced increases the Poisson's ratio to approach incompressibility. However, a saturated sediment also begins to loose cohesion between grains, as water both lubricates movement and forces grains apart, thus the shear strength decreases with increased moisture content (Smith, 1981), resulting in a soft sediment.

3. Fossil description

The fossil is a natural cast and is hence seen in positive relief (Fig. 3). The track has three prominent digits, and was described to be a left track, with a 'web-like' structure occurring prominently between the central and right digits (II and III), and less pronounced between the central and left digits (III and IV) (Lockley et al., 2004). This interdigital structure appears as a 'platform' when viewed in profile (Fig. 4). A reversed digit is also present at the posterior of the track at an angle to the central axis. The central part of the foot, where the digits converge, is not impressed clearly. Track length is ~95 mm from tip of Digit III to the tip of the reversed digit; and track width is also ~95 mm from tip of Digit II to tip of Digit IV.

Shallow sinuous asymmetric ripples are present on the surface, more visible in the profile image taken from the laser scan than the original natural cast (Fig. 5). Small circular impressions are also present, and are concentrated on the crests of the ripples. These impressions are distributed unevenly over the ripples, occurring more on the stoss side of the ripple (Figs. 3 and 5).

4. Simulated track description

The finite element track displayed features consistent with wet, soft sediment deformation, including displacement rims and an uneven surface (Manning, 1999). Of particular interest with regard to this paper, is the form of the displacement rim between Digits III and IV. Here, the sediment is stepped (Figs. 6 and 7), creating a visible line between the digits from the tip of Digit IV to approximately half way along Digit III. Additionally, there is a smaller ridge of similar form between Digits III and II, though this structure is less pronounced, extending from digit tip to digit tip.

An advantage to the FEA model is to easily look within the sediment and view surfaces at any level within the 3D volume. At 50 cm depth below the track surface, and though the track has become faint by this depth, being less than 1 cm in relief, there is still a distinct failure structure between the digits comparable to the surface track (Fig. 8).

A second FEA track was produced with a higher shear strength (u=65 kN/m^2, approximating a 'firm' clay). However, this track did not show any signs of failure between digits.

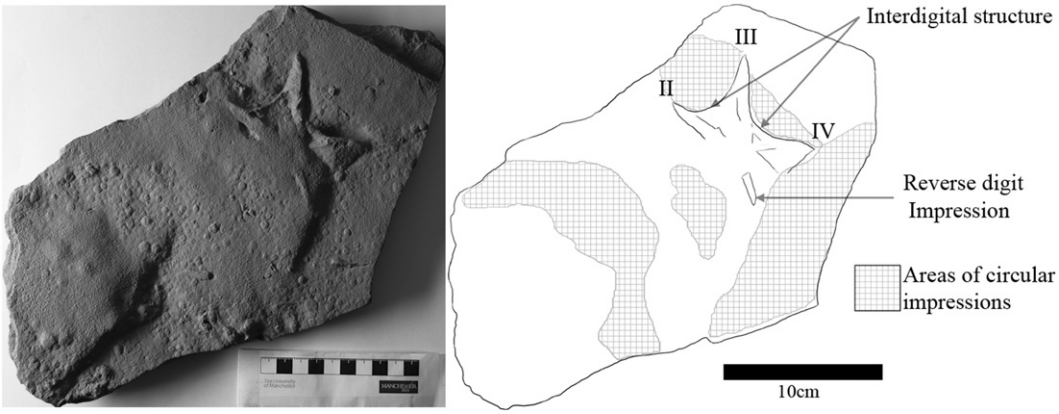

Fig. 3. Photograph and outline drawing of cast of CU-MWC224.4 highlighting interdigital features, locations of circular impressions and digits of track. Scale bar = 10 cm, light source from the left.

Also, two further experiments were undertaken to investigate the effects of interdigital angle. In the first experiment, Digit IV was rotated to create a smaller interdigital angle (25°), and a narrower foot, whilst in the second experiment the procedure was reversed and the digit was rotated back to produce a larger interdigital angle (95°) (Fig. 9). Substrate conditions were identical to the original experimental

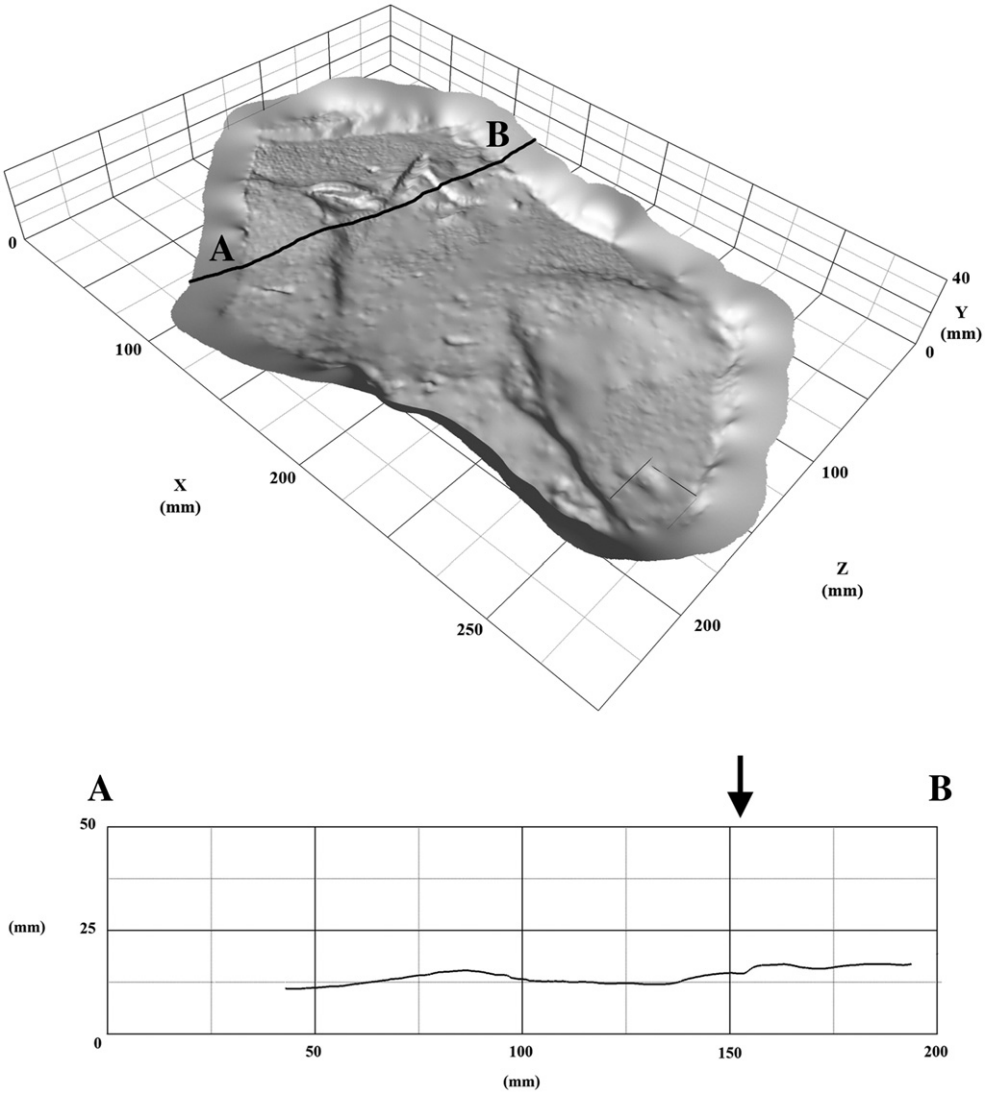

Fig. 4. Laser scanned surface (overturned) and profile of CU-MWC224.4. Arrow above profile indicates structure referred to as 'webbing impression.' Light in upper image is from the left.

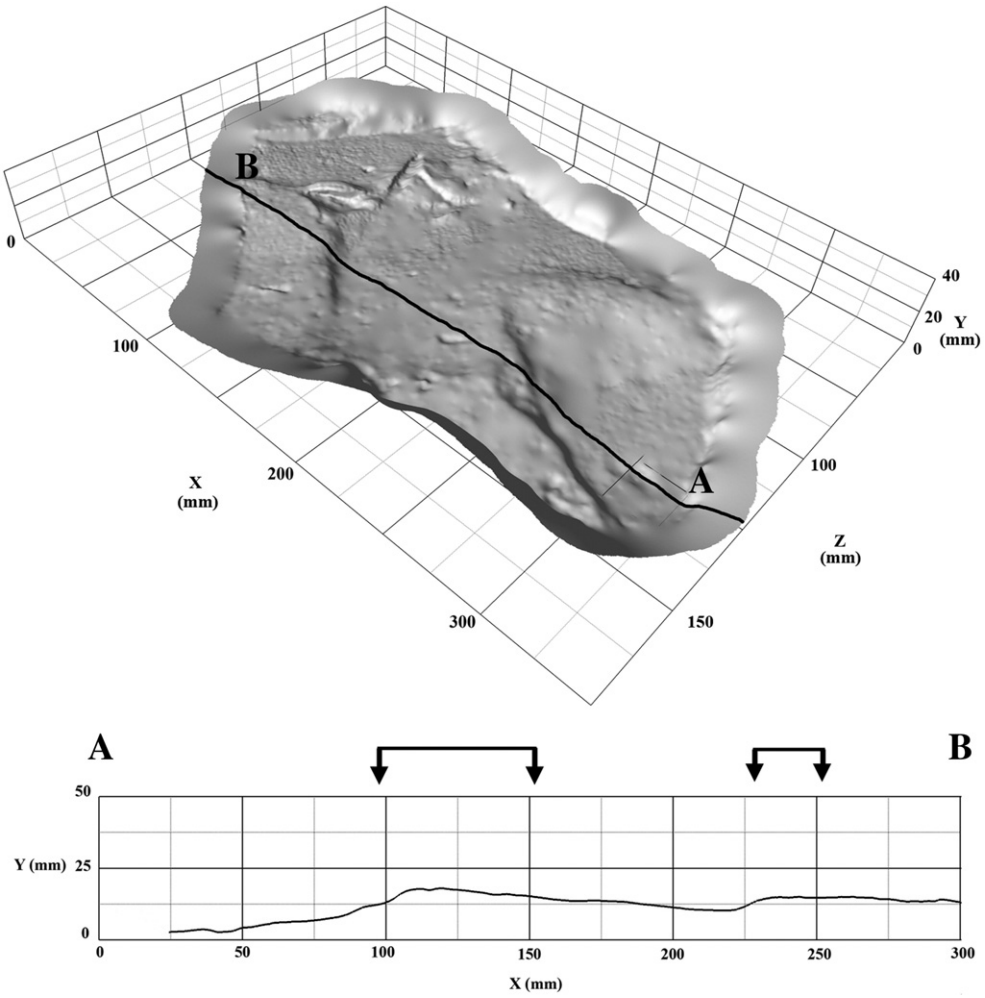

Fig. 5. Laser scanned surface (overturned) and profile of CU-MWC224.4. Arrows above profile indicate areas of concentrated raindrop impressions. Light in upper image is from the left.

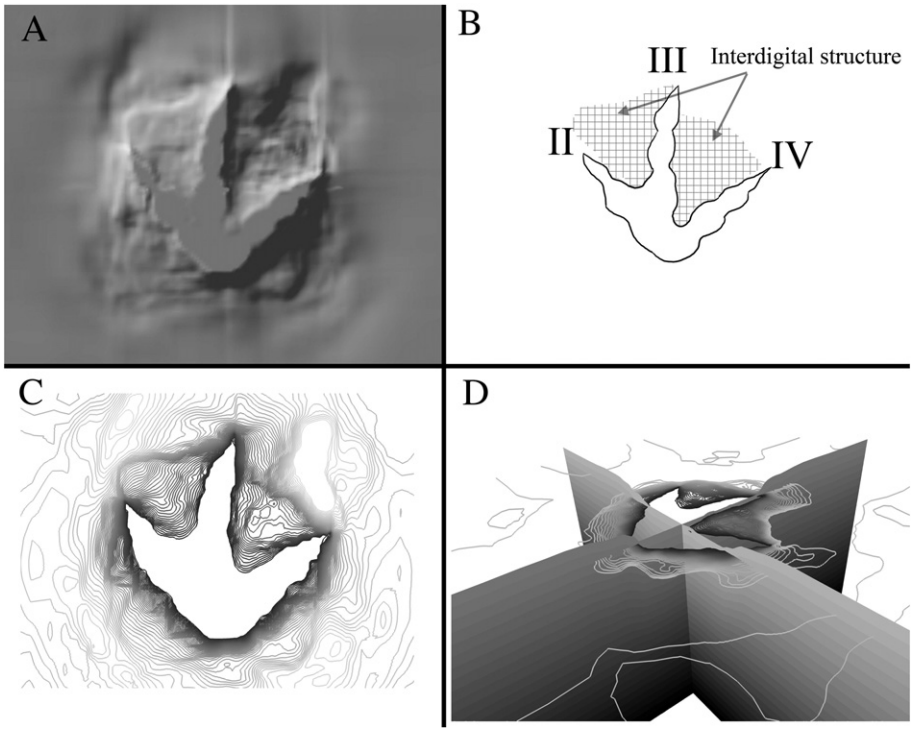

Fig. 6. A) Simulated track formed in virtual substrate comparable to wet, soft sediment, light source is from the lower right. B) Interdigital structures are labelled. C) Two-dimensional map of isolines of displacement, closer contours indicate steeper gradient. Note steepest gradients at extents of interdigital structures. D) Location of 2D displacement map relative to 3D volume.

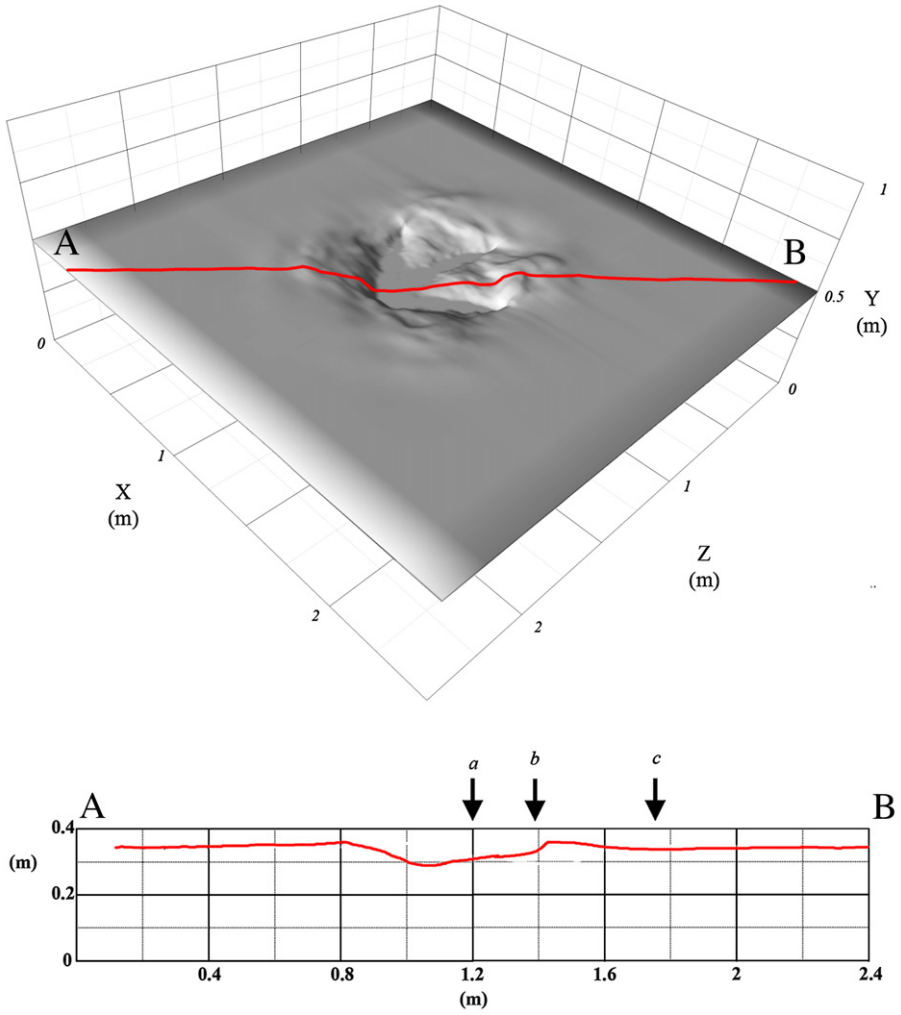

Fig. 7. Surface track and cross-sectional profile of finite element track. Arrows labelled 'a' 'b' and 'c' mark; the start of sediment displacement beyond the foot–sediment interface, the 'stepped' structure in the displacement and the extremity of the displacement rim respectively.

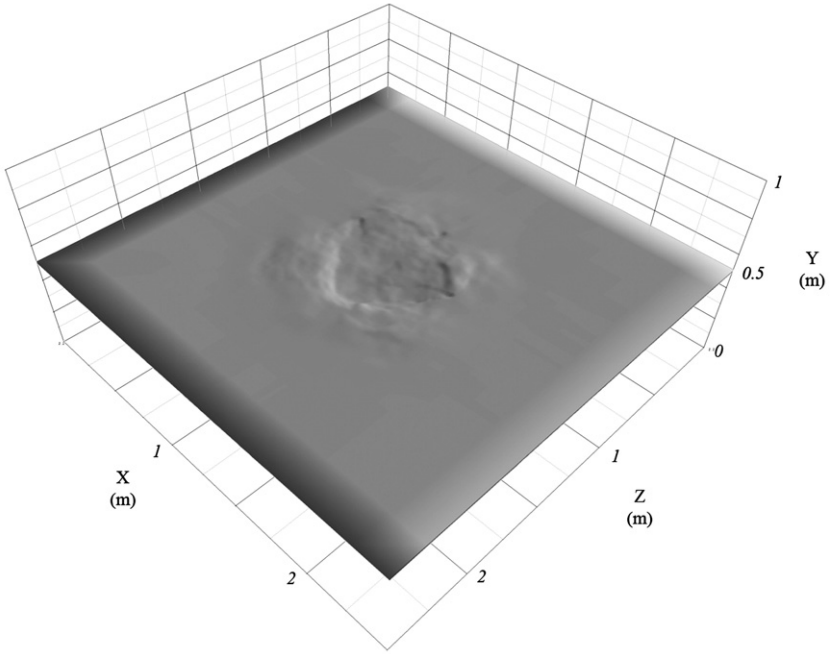

Fig. 8. Surface at 50 cm depth below surface seen in Fig. 7.

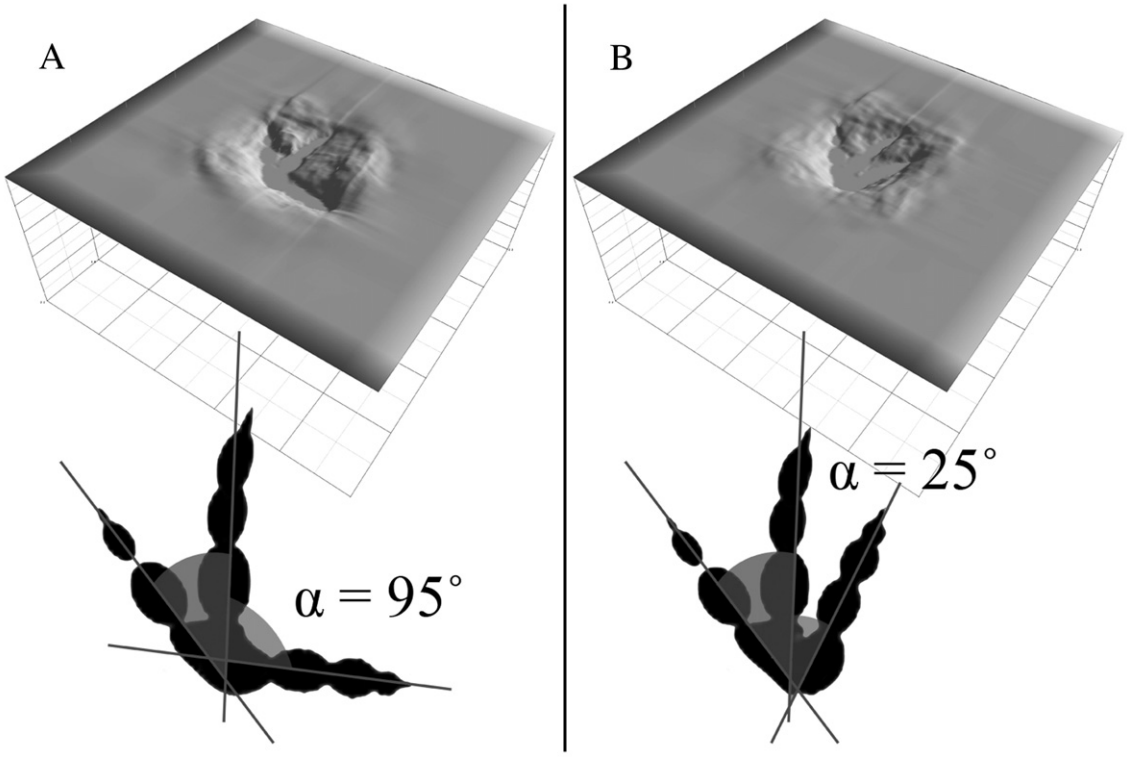

Fig. 9. Experiments in which wider (A) and narrower (B) interdigital angles between Digits III and IV were used.

conditions. In neither experiment was a feature analogous to 'webbing' visible.

5. Discussion

The fossil track CU-MWC224.4 has previously been interpreted as being generated by a semi-palmate (webbed) bird foot (Lockley et al., 2004). The surface upon which the track is located is rippled and covered with circular impressions interpreted as rain pitting. The ripples are shallow and asymmetric, which are consistent with the palaeoenvironmental interpretation of shallow water at the edge of a channel. The raindrops occur almost exclusively on the crests of ripples, implying some difference between the crests and the troughs affecting the formation and/or preservation of raindrop impressions. We propose standing water of a few mm, which occupied the topographic lows, leaving the drier ripple crests exposed. Reineck and Singh (1980, p. 61) suggest that raindrops falling on a freshly exposed rippled surface will form better impact impressions on the relatively drier crests than the wet troughs. This is supported by the presence of raindrops extending further over the stoss side of the ripples, creating a palaeo-waterline. The interpreted environmental setting is of wet, waterlogged fine-grained sediment located at the edge of flowing water, supporting the original interpretation (Lockley et al., 2004).

Taking this into account, the finite element model was created with similar properties to a fine-grained, saturated substrate. The indentation of a tridactyl foot resulted in a track with a feature very similar to the 'webbing' described in CU-MWC224.4. This structure formed through sediment failure as the sediment was pushed up between the toes, and then collapsed. This 'interdigital shear' was described by Manning (1999, 2004), and represents a peak of stress within the sediment that causes shearing. The interdigital shear was present in subsurface deformation to a considerable depth.

When interdigital angle was increased or decreased for Digits III and IV, the simulation did not produce web-like structures. This implies a specific IDA in tridactyl feet conducive to forming web-like structures through sediment failure, in this case the resultant 'webbed' track had an IDA of 50° where 'webbing' formed (between Digits III and IV). It should be noted here that the fossil track CU-MWC224.4 has interdigital angles of 50° and 90° between Digits II and III and III and IV respectively, and the prominent webbing is only located between Digits II and III. Where the IDA is large, a much smaller structure is observed.

Given the palaeoenvironment in which the track was formed, we propose that rather than webbing, these structures are a function of sedimentary environment, foot morphology, digit position, and rheology. Such a scenario accounts for the trackway described by Lockley et al. (2004, Fig. 15a), where only two of the three tracks in a single trackway appear to have 'webbing', and this 'webbing' varies between individual tracks. Alternatively, in a firm substrate it is conceivable that a webbed foot may leave no evidence of webbing as the weight bearing digits support the web above the substrate surface. If this were the case however, the tracks would be considerably shallower.

The presence of an algal or microbial mat on the surface of the sediment would alter the properties of the upper few mm. Providing the foot did not puncture the substrate surface, the microbial mat may provide adhesion between grains to prevent the failure seen in the FEA models. If however the foot did puncture the mat, the adhesive properties offered would hold the platformed sediment in place, potentially exaggerating the 'webbed' effect.

The ideal conditions for sediment failure to produce a 'webbed' track (wet, soft, fine-grained sediment), coincide with the conditions in which one would expect waterbirds with palmate feet to be found, leading to inherent complications in interpreting palmate tracks. Sediment deformation, however, may be considered the most likely/parsimonious explanation in specific cases, especially when 'webbed' tracks would extend the phylogenetic range of palmate birds, or would imply the presence of interdigital webbing in groups such as dinosaurs that currently have no supporting evidence for such an interpretation.

6. Conclusions

Using new methods including FEA and high resolution laser scanning, we have shown the mechanism by which a track can be produced with a palmate or semi-palmate morphology, even when the foot itself is not webbed. In this case, the example track used indicated a waterlogged substrate. This is supported with the FEA simulations in which low shear strength and high Poisson's ratio (soft and incompressible) produced 'semi-palmate' tracks.

Saturated, soft, fine-grained substrate is ideal for this type of sediment failure, but is also the predicted sediment in which to find palmate tracks. This means that we present only an alternative hypothesis, rather than a replacement. However, the implications of this apply to all palmate/semi-palmate tracks in the fossil record, suggesting care should be taken when describing such tacks in the future. Descriptions of track features should look for direct evidence of webbing (e.g. skin impression) or sediment failure, especially when the tracks occur outside the phylogenetic range of palmate birds as defined by other fossils.

Acknowledgements

We would like to thank NERC for providing a grant to Falkingham (ref: NER/S/A/2006/14033), P. Larson for access to cast material, and Karl Bates for constructive comments and discussion during the writing of the paper. Also Finn Surlyk, Jesper Milàn, and Brent Breithaupt for constructive reviews of the manuscript. The finite element simulations were carried out using HECToR, through EPSRC project EP-F055595-1.

References

Allen, J.R.L., 1989. Fossil vertebrate tracks and indenter mechanics. Journal of the Geological Society 146, 600–602.

Allen, J.R.L., 1997. Subfossil mammalian tracks (Flandrian) in the Severn Estuary, SW Britain: mechanics of formation, preservation and distribution. Philosophical Transactions of the Royal Society of London. Series B, Biological Sciences 352, 481–518.

Bates, K.T., 2006. The application of Light Detection and Range (LIDAR) imaging to vertebrate ichnology and geoconservation (M. Phil Theses), University of Manchester, Manchester, 347 pp.

Bates, K.T., Rarity, F., Manning, P.L., Hodgetts, D., Vila, B., Oms, O., Galobart, À., Gawthorpe, R., 2008. High-resolution LiDAR and photogrammetric survey of the Fumanya dinosaur tracksites (Catalonia): implications for the conservation and interpretation of geological heritage sites. Journal of the Geological Society, London 165, 115–127.

Bowles, J.E., 1968. Foundation Analysis and Design. McGraw-Hill, New York. 659 p.

Burnet, D.S., 1987. Finite Element Analysis from Concepts to Applications. Addison-Wesley Publishing Company, Reading, M.A. 844 pp.

Craig, R.F., 1997. Soil Mechanics. Chapman & Hall, London. 485 pp.

Day, J.J., Norman, D.B., Gale, A.S., Upchurch, P., Powell, H.P., 2004. A Middle Jurassic dinosaur trackway site from Oxfordshire, UK. Palaeontology 47, 319–348.

Fervers, C.W., 2004. Improved FEM simulation model for tire–soil interaction. Journal of Terramechanics 41, 87–100.

Henderson, D.M., 2006. Simulated weathering of dinosaur tracks and the implications for their characterization. Canadian Journal of Earth Sciences 43, 691–704.

Johnson, K., Lemcke, P., Karunasena, W., Sivakugan, N., 2006. Modelling the load-deformation response of deep foundations under oblique loading. Environmental Modelling & Software 21, 1375–1380.

Karafiath, L.L., Nowatzki, E.A., 1978. Soil mechanics for off-road vehicle engineering. Series on Rock and Soil Mechanics. Trans Tech publications, Aedermannsdorf. 515 pp.

Kim, J.Y., Kim, S.H., Kim, K.S., Lockley, M., 2006. The oldest record of webbed bird and pterosaur tracks from South Korea (Cretaceous Haman Formation, Changseon and Sinsu Islands): more evidence of high avian diversity in East Asia. Cretaceous Research 27, 56–69.

King, M.J., Benton, M.J., 1996. Dinosaurs in the Early and Mid Triassic? — The footprint evidence from Britain. Palaeogeography, Palaeoclimatology, Palaeoecology 122, 213–225.

Lim, J.-D., Zhou, Z., Martin, L.D., Baek, K.S., Yang, S.Y., 2000. The oldest known tracks of web-footed birds from the Lower Cretaceous of South Korea. Naturwissenschaften 87, 256–259.

Lockley, M., Rainforth, E., 2002. The tracks record of Mesozoic birds and pterosaurs: an ichnological and paleoecological perspective. In: Chiappe, L., Witmer, L.M. (Eds.), Mesozoic Birds above the Heads of Dinosaurs. University of California Press, Berkeley, pp. 405–418.

Lockley, M.G., Nadon, G., Currie, P.J., 2004. A diverse dinosaur-bird footprint assemblage from the Lance Formation, Upper Cretaceous, Eastern Wyoming: implications for ichnotaxonomy. Ichnos 11, 229–249.

Manning, P.L., 1999. Dinosaur track formation, preservation and interpretation: fossil and laboratory simulated dinosaur track studies. Ph.D Thesis, University of Sheffield (England).

Manning, P.L., 2004. A new approach to the analysis and interpretation of tracks: examples from the dinosauria. In: McIlroy, D. (Ed.), The Application of Ichnology to Palaeoenvironmental and Stratigraphic Analysis. Special Publications, Geological Society, London, pp. 93–123.

Manning, P.L., 2008. *T. rex* speed trap. In: Carpenter, K., Larson, P.L. (Eds.), *T. rex* Symposium Volume. Indiana University Press, Bloomington, pp. 205–231.

Manning, P.L., Margetts, L., Leng, J., Smith, I.M., Falkingham, P.L., in review. Using computer simulation to gain a new perspective on dinosaur trackways.

Margetts, L., Smith, I.M., Leng, J., Manning, P.L., 2006. Parallel three-dimensional finite element analysis of dinosaur trackway formation. In: Schweiger, H.F. (Ed.), Numerical Methods in Geotechnical Engineering. Taylor & Francis, London, pp. 743–749.

Milàn, J., 2006. Variations in the morphology of emu (*Dromaius novaehollandiae*) tracks reflecting differences in walking pattern and substrate consistency: ichnotaxonomic implications. Palaeontology 49, 405–420.

Milàn, J., Bromley, R.G., 2006. True tracks, undertracks and eroded tracks, experimental work with tetrapod tracks in laboratory and field. Palaeogeography, Palaeoclimatology, Palaeoecology 231, 253–264.

Milàn, J., Bromley, R.G., 2008. The impact of sediment consistency on track and undertrack morphology: experiments with emu tracks in layered cement. Ichnos 15, 19–27.

Milàn, J., Clemmensen, L.B., Bonde, N., 2004. Vertical sections through dinosaur tracks (Late Triassic lake deposits, East Greenland) — undertracks and other subsurface deformation structures revealed. Lethaia 37, 285–296.

Nakashima, H., Wong, J.Y., 1993. A three-dimensional tire model by the finite element method. Journal of Terramechanics 30, 21–34.

Nakashima, H., Oida, A., 2004. Algorithm and implementation of soil–tire contact analysis code based on dynamic FE-DE method. Journal of Terramechanics 41, 127–137.

Rayfield, E.J., 2004. Cranial mechanics and feeding in *Tyrannosaurus rex*. Proceedings of the Royal Society of London. Series B, Biological Sciences 271, 1451–1459.

Rayfield, E.J., 2005. Using finite-element analysis to investigate suture morphology: a case study using large carnivorous dinosaurs. Anatomical Record. Part A, Discoveries in Molecular Cellular and Evolutionary Biology 283A, 349–365.

Rayfield, E.J., 2007. Finite element analysis and understanding the biomechanics and evolution of living and fossil organisms. Annual Review of Earth Planetary Sciences 35, 541–576.

Rayfield, E.J., Norman, D.B., Horner, C.C., Horner, J.R., Smith, P.M., Thomason, J.J., Upchurch, P., 2001. Cranial design and function in a large theropod dinosaur. Nature 409, 1033–1037.

Reineck, H.E., Singh, I.B., 1980. Depositional Sedimentary Environments. Springer Verlag, Berlin. 542 pp.

Sarjeant, W.A.S., 1967. Fossil footprints from the Middle Triassic of Nottingham and the Middle Jurassic of Yorkshire. Mercian Geologist 3, 269–282.

Scheiner, S., Pichler, B., Hellmich, C., Eberhardsteiner, J., 2006. Loading of soil-covered oil and gas pipelines due to adverse soil settlements — protection against thermal dilatation-induced wear, involving geosynthetics. Computers and Geotechnics 33, 371–380.

Shoop, S.A., 2001. Finite element modelling of tire–terrain interaction. ERDC/CRREL TR-01-16, U.S. Army Corps of Engineers, Engineer Research and Development Center.

Shoop, S., Kestler, K., Haehnel, R., 2006. Finite element modeling of tires on snow. Tire Science and Technology 34, 2–37.

Smith, M.J., 1981. Soil Mechanics. George Godwin, London. 168 pp.

Smith, I.M., Griffiths, D.V., 2004. Programming the Finite Element Method. Wiley, Chichester. 628 pp.

Yang, S.Y., Lockley, M., Greben, R., Erikson, B.R., Lim, S.Y., 1995. Flamingo and duck-like bird tracks from the Late Cretaceous and Early Tertiary: evidence and implications. Ichnos 4, 21–34.

You, H.-L., Lamanna, M.C., Harris, J.D., Chiappe, L.M., O'connor, J., Jl, S.-A., Lu, J.-C., Yuan, C.-X., Li, D.-Q., Zhang, X., Lacovara, K.J., Dodson, P., Ji, Q., 1995. A nearly modern amphibious bird from the early cretaceous of northwestern China. Science 312 (5780), 1640–1643.